Valence Change of A-Site Mn by A-Site Doping in La1–xNaxMn3Ti4O12

Cite as:
Tohyama, T., Senn, M. S., Saito, T., Chen, W., Tang, C. C., Attfield, J. P., & Shimakawa, Y. (2013). Valence Change of *A′*-Site Mn by *A*-Site Doping in $La_{1-x}Na_xMn_3Ti_4O_{12}$. *Chemistry of Materials*, 25(2), 178-183.

Manuscript received: 02/10/2012; Accepted: 19/12/2012; Article published: 08/01/2013

Valence Change of *A′*-Site Mn by *A*-Site Doping in $La_{1-x}Na_xMn_3Ti_4O_{12}$**

Takenori Tohyama,[1] Mark S. Senn,[2] Takashi Saito,[1] Wei-tin Chen,[1] Chiu C. Tang,[3] J. Paul Attfield[2] and Yuichi Shimakawa[1,4,*]

[1]Institute for Chemical Research, Kyoto University, Uji, Kyoto 611-0011, Japan.

[2]EaStCHEM, School of Chemistry and Centre for Science at Extreme Conditions, Joseph Black Building, University of Edinburgh, West Mains Road, Edinburgh, EH9 3JJ, UK.

[3]Diamond Light Source Ltd., Harwell Science and Innovation Campus, Didcot, Oxfordshire OX11 0DE, UK.

[4]Japan Science and Technology Agency, CREST, Uji, Kyoto 611-0011, Japan.

[*]Corresponding author; Y.S. e-mail: shimak@scl.kyoto-u.ac.jp

[**]This work was performed under the Strategic Japanese-UK Cooperative Program by Japan Science and Technology Agency (JST) and Engineering and Physical Sciences Research Council (EPSRC). The synchrotron X-ray diffraction experiments were performed with the approval of the Diamond Light Source in the UK. The work was partly supported by Grants-in-Aid for Scientific Research (Grant Nos. 19GS0207 and 22740227), by the Global COE Program "International Center for Integrated Research and Advanced Education in Materials Science" (No. B-09), by the Project of Integrated Research on Chemical Synthesis from the Ministry of Education, Culture, Sports, Science and Technology (MEXT) of Japan, and by the JST CREST program. Support was also provided by EPSRC and the Leverhulme Trust, United Kingdom.

Graphical abstract:

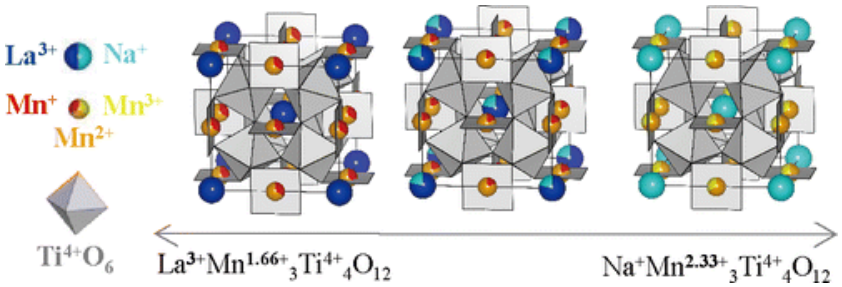

Keywords:
A-site-ordered perovskites, high-pressure synthesis, resonant X-ray diffraction, magnetic properties, valence states of cations

Abstract

A-site-ordered perovskites $La_{1-x}Na_xMn_3Ti_4O_{12}$ with (x = 0, 0.5, 1) were synthesized under high-pressure and high-temperature conditions, and their crystal structures and magnetic properties were investigated. Mn/Ti occupancies at the *B*-site was also examined by using resonant X-ray scattering, and the results confirm that they were stoichiometrically synthesized with high Mn/Ti site selectivity. Substituting Na^+ for some of the La^{3+} changed the valence state of the *A*'-site Mn but not of the *B*-site Ti, and thus the compositions of the synthesized samples are expressed as $La_{1-x}Na_xMn^{(5+2x)/3}{}_3Ti^{4+}{}_4O_{12}$. The magnetic behaviors change from antiferromagnetic to spin-glass like behavior according to the valence states of *A*'-site Mn.

Introduction

Perovskite oxides with a chemical formula ABO_3 are actively studied because they show a wide variety of chemical and physical properties. The properties, especially those in electric transport and magnetism, are often attributed to interactions between transition-metal cations at the *B*-site (via oxygen ions). When 3/4 of the *A*-sites of a simple perovskite is occupied by another transition-metal cation, *A*-site-ordered perovskites, $AA'_3B_4O_{12}$, can be stabilized (Fig. 1). The compounds offer opportunities to see intriguing properties due to the additional *A'*-*A'* and *A'*-*B* interactions.[1,2] In $CaCu_3(Sn,Ti,Ge)_4O_{12}$, for example, one finds a very unusual *A'*-*A'* magnetic interaction in which either ferromagnetism or antiferromagnetism of the *A'*-site Cu^{2+} spins is stabilized by changing the non-magnetic *B*-site cations.[3, 4, 5] In $ACu_3Fe_4O_{12}$ ($A = La^{3+}$, Bi^{3+}), intersite charge transfer between the *A'*-site Cu and the *B*-site Fe ($Cu^{2+} + Fe^{+3.75} \rightarrow Cu^{3+} + Fe^{3+}$) causes a significant change in the unit-cell volume as well as paramagnetic-to-antiferromagnetic and metal-to-insulator transitions.[6, 7]

The *A* site in $AA'_3B_4O_{12}$, like that in simple perovskites, accommodates alkaline metals, alkaline-earth metals, and lanthanides. The interactions of the transition-metal ions and the resultant properties of $AA'_3B_4O_{12}$ can also be tuned by substitution at the *A*-site cation. The substitution of La^{3+}/Bi^{3+} for Ca^{2+} at the *A*-site, indeed, changes semiconducting $CaCu_3Mn_4O_{12}$[8] to metallic $(La/Bi)Cu_3Mn_4O_{12}$[9,10] with spin-polarized conduction carriers and the doped compounds show large magnetoresistance. The aliovalent substitution at the *A* site affects the valence state of the *B*-site transition-metal cation and produces the mixed valency in Mn.

Large number of the *A*-site ordered perovskites with Cu at the *A'* site have been found and some with Mn at the *A'* site are also known. Mn at the *A'*-site usually shows a trivalent state, as seen in $AMn^{3+}{}_3Mn_4O_{12}$ (*A* = Na^+, Ca^{2+}, La^{3+}, Bi^{3+})[11,12,13] and $A^{3+}Mn^{3+}{}_3Al^{3+}{}_4O_{12}$, and the square-planer coordination with oxygen appeared to stabilize the Jahn-Teller active Mn^{3+} ions.[14, 15] Recently, however, analysis of the synchrotron X-ray diffraction, X-ray absorption spectrum, and magnetization of $LaMn_3Ti_4O_{12}$ indicated that the compound has a nominal composition of $La^{3+}Mn^{1.66+}{}_3Ti^{4+}{}_4O^{2-}{}_{12}$ with an unusually low-valence Mn ion apparent at the *A'* site.[16] Mn with a valence lower than +2 is very rare for oxides, therefore we are interested how the *A*'-site Mn valence would be affected by changing *A*-site ion. In this study we focus on a $La_{1-x}Na_xMn_3Ti_4O_{12}$ system, where the Na^+ substitution for La^{3+} at the *A* site effectively causes the hole doping.

In discussing the cation-valence states in the $AMn_3Ti_4O_{12}$ system in detail, it is very important to determine not only the overall stoichiometry but also the precise site occupancies of each ions, because the valence states of the *A*'-site Mn can easily be adjusted by the Mn/Ti mixing. However, to clarify such Mn/Ti mixing over the *A'* and *B* sites in $La_{1-x}Na_xMn_3Ti_4O_{12}$ is not easy to explore from the structure refinements using normal (non-resonant) X-ray or neutron diffraction techniques because Ti and Mn have similar X-ray scattering amplitudes (atomic numbers, Z = 22 for Ti and 25 for Mn) and neutron scattering factors (b = -3.37 and -3.73 fm for Ti and Mn, respectively). In this study then we adopt resonant X-ray scattering (RXS) technique, which enables to distinguish the elements with close atomic numbers like Mn and Ti by making contrast between their anomalous scattering factors *f'* and *f"*.

With the RXS results, we can clarify the precise chemical compositions and site occupancies in $La_{1-x}Na_xMn_3Ti_4O_{12}$, and thus can discuss the valence states of the *A'*-site Mn and *B*-site Ti in the compounds. The obtained results strongly suggest the *A*-site substitution effectively causes the doping only into the *A'*-site Mn. The valence states of Mn at the *A'* site are also discussed from the magnetic behaviors of Mn ions.

The *A*-site doping effects into the *A*'- and *B*-sites are compared with those in other *A*-site ordered double perovskite structure oxides.

Experimental Section

Polycrystalline samples with nominal compositions $La_{1-x}Na_xMn_3Ti_4O_{12}$ (x = 0, 0.5, and 1), were synthesized under high-pressure and high-temperature conditions. The starting materials (La_2O_3, Na_2O_2, Mn_2O_3, Ti_2O_3, and TiO_2) were weighed out in stoichiometric proportions, mixed and packed into cylindrical gold capsules 2.8 mm in diameter before being pressed isotropically with a cubic-anvil-type apparatus. The synthesis conditions, 9 GPa and 1273 K, maintained for 30 minutes. We also made $LaMn_3Ti_3MnO_{12}$ and $LaMn_3Ti_3ScO_{12}$ as references in the similar manner.

Synchrotron powder X-ray diffraction for both resonant (λ=1.898161 Å) and non-resonant (λ=0.82716 Å) conditions was performed on a diffractometer at I11, Diamond. The samples were mounted on the outside of a 0.5mm diameter capillaries using organic grease as an adhesive. In RXS, wavelength tuned to the *K*-edge of one of the metals may be used to induce large anomalous scattering changes for that element, providing useful contrast for occupancy refinements. An energy just below the *K*-edge of the lighter element would ideally be used to minimize sample absorption, but in this case the Ti *K*-edge is below the practical range for the I11 diffractometer. Therefore, the Mn *K*-edge was used for the experiment. The spectra were measured by simultaneously scanning the monochromator and the undulator gap and the edge was found to be at E = 6547.0 keV. The beam energy was reduced to 15 eV below this value for the diffraction experiments and determined from a Si standard to be λ = 1.898161 Å, E = 6529.6 eV. The samples were measured for approximately 8 hours each at this wavelength in Debye-Scherrer geometry in the 2θ range from 0^o to 150^o. Values of the anomalous dispersion coefficients f' (実験に用いた値) and f'' (実験に用いた値) were taken from a standard source. [19] The combined analysis of the resonant and non-resonant X-ray diffraction data was carried out by using the Topas program.[17].

Magnetic properties of the samples were measured using a commercial SQUID magnetometer (MPMS, Quantum Design). Temperature dependence of magnetic susceptibility was measured in a 1kOe magnetic field.

Experimental Results

(i) Crystal structure analysis

The main phase of each sample was confirmed to be an *A*-site-ordered perovskite structure with the space group *Im*-3. In the refinement we initially assigned

the atomic positions as *A*(0, 0, 0), Mn(0, 0.5, 0.5), Ti(0.25, 0.25, 0.25), and O(*x*, *y*, 0), but the result did not give a good fit and gave large isotropic atomic displacement parameters for the *A*'-site Mn; U_{iso} was 0.049 for $LaMn_3Ti_4O_{12}$, 0.079 for $La_{0.5}Na_{0.5}Mn_3Ti_4O_{12}$, and 0.018 $Å^2$ for $NaMn_3Ti_4O_{12}$. We then refined the crystal structures with a split site model in which the positions of *A*'-site Mn ions are displaced from the special 6*b* (0, 0.5, 0.5) position to 12*e* (0, *y*, 0.5). This greatly improved the refinement results, decreasing the R_{wp} value for $LaMn_3Ti_4O_{12}$, for example, from 7.90 to 6.32 %. Similar improvement in the refinements was obtained using a model with large anisotropic thermal vibration parameters β_{ij} for Mn ions. The fits obtained with the two models did not differ significantly, but we use the split site model as it is more physically realistic. The results of the final refinements are listed in Table 1 and a typical refinement result in the diffraction pattern is shown in Fig. 2 for $LaMn_3Ti_4O_{12}$.

No anomalies in the occupancies at the oxygen sites were observed, suggesting oxygen stoichiometries in any of the samples. No obvious cation deficiencies at the A-site were also detected, but the refined *A*-site occupancies in $La_{0.5}Na_{0.5}Mn_3Ti_4O_{12}$ differed slightly from the nominal ones, giving an *A*-site composition $La_{0.781(1)}Na_{0.219}$. In Fig.3, the lattice constants of $La_{1-x}Na_xMn_3Ti_4O_{12}$ are plotted against *x* values. The change of the constants is linear according to the change of *x* and thus it is consistent with Vegard's law. This consistency indicates that the solid solution of $La_{1-x}Na_xMn_3Ti_4O_{12}$ with the refined compositions was successfully synthesized. The refinements for the *A'*-site Mn gave no unusual results suggesting the full occupancy of Mn at the site. It is also noted that the refined Mn/Ti occupancies listed in Table 1 suggest quite small amount of Mn incorporation into the *B* site. The refined values are 0.943(4)/0.057 for $NaMn_3Ti_4O_{12}$, 1.039(4)/-0.039 for $La_{0.5}Na_{0.5}Mn_3Ti_4O_{12}$, 0.992(3)/0.008 for $LaMn_3Ti_4O_{12}$. This is also consistent with the observations of amounts of secondary impurities. Although the synthesized samples sometimes contain small amounts of impurities like TiO_2 and $La(Mn,Ti)O_3$ perovskites, the amounts of those phase were always less than 5%. Thus we can conclude that the Mn/Ti mixing in $La_{1-x}Na_xMn_3Ti_4O_{12}$ should be insignificant and almost negligible.

With the structure refinement results, we can calculate the bond valence sum (BVS)[18] of cations and the results are also listed in Table 1. One sees that BVS for the *A*-site cations respectively are 1.16 and 3.09 for the $x = 0.0$ and 1.0 samples, confirming the successful synthesis of the end composition samples. It should also be noted that the BVS for the *A*'-site Mn changes from 2.20 to 1.79 to 1.76 with increasing *x* form 0.0 to 1.0, whereas that for the *B*'-site Ti does not differ significantly. Therefore, the valence states for the *B*-site Ti appear to be +4 for all the samples, and given that the *B* sites are

occupied by only Ti^{4+} (which implies that the Mn/Ti mixing is negligible as we saw above), the refinement results give $Na^{+}Mn^{2.33+}{}_3Ti^{4+}{}_4O_{12}$ (x = 0.0), $(La_{0.781}Na_{0.219})^{2.56+}Mn^{1.81+}{}_3Ti^{4+}{}_4O_{12}$ (x = 0.5), and $La^{+}Mn^{1.66+}{}_3Ti^{4+}{}_4O_{12}$ (x = 1.0). The obtained change in the BVS for Mn at the *A'* site seen in the Table 1 is quite consistent with the estimation from the simple ionic model.

(ii) Transport and Magnetic property measurements

All the $La_{1-x}Na_xMn_3Ti_4O_{12}$ samples were electrically insulating, which strongly suggest that all the Ti at the octahedral *B* site are tetravalent. Although they contain Mn ions with mixed valence states at the *A*'-site, their 3*d* electrons are localized. The square-planar MnO_4 units are isolated with each other due to the peculiar orthogonal alignment, which may account for the localization.

Here the *B* sites in $La_{1-x}Na_xMn_3Ti_4O_{12}$ are occupied by non-magnetic Ti^{4+}, and thus the magnetic properties originate from the interactions of Mn spins at the *A'*-site. Temperature dependence of magnetic susceptibility and inverse susceptibility for $La_{1-x}Na_xMn_3Ti_4O_{12}$ are shown in Fig. 4. The susceptibility above 150 K obeys the Curie-Weiss law $\chi = C/(T-\theta)$, and the Curie constants and the Weiss temperatures obtained from the fits are listed in Table2. The Weiss temperatures are all negative, suggesting antiferromagnetic interactions between the magnetic spins, and the absolute values of θ increases with increasing Na doping at the *A*-site. As shown in magnified views of the susceptibility data at low temperature (Fig. 4), the anomalies are seen at 5 K for $LaMn_3Ti_4O_{12}$, 9 K for $(La_{0.781}Na_{0.219})Mn_3Ti_4O_{12}$, and 8 K for $NaMn_3Ti_4O_{12}$. Given the magnetic transitions occur at those temperatures (T_m), $|\theta|/T_m$ ratios respectively are 7, 6, and 10, indicating that the antiferromagnetic interactions are highly frustrated.

In Table 2, we show the magnetic moments calculated from the Curie constants. If the mixed valence states of Mn at the *A'* site are due to a mixture of Mn^{+}, Mn^{2+}, and Mn^{3+} ions, the effective magnetic moments of those ions with high-spin configurations agree well with those estimated from the Curie constants. Thus, the magnetic results also support that Mn ions at the *A'* site produce local spins and that those valence states of Mn change with changing the *A*-site composition *x*.

Discussion

The all experimental results strongly suggest that the *A*-site doping causes the change in the valence state of the *A*'-site Mn but does not affect the valence state of the *B*-site Ti; $Na^{+}Mn^{2.33+}{}_3Ti^{4+}{}_4O_{12}$ (x = 0.0), $(La_{0.781}Na_{0.219})^{2.56+}Mn^{1.81+}{}_3Ti^{4+}{}_4O_{12}$ (x = 0.5),

and $La^{+}Mn^{1.66+}{}_3Ti^{4+}{}_4O_{12}$ (x = 1.0). The behavior differs completely from those seen in other $ACu_3B_4O_{12}$ double-perovskite oxides containing Cu at the *A* site. In $ACu_3Mn_4O_{12}$ ($A = Ca^{2+}$, La^{3+}/Bi^{3+}) the change in the valence of the *A*-site cation is compensated by the change in the valence of only the *B*-site cations and does not affect the valence of the *A*'-site Cu, *i.e.*, $Ca^{2+}Cu^{2+}{}_3Mn^{4+}{}_4O_{12}$[8] and $(La/Bi)^{3+}Cu^{2+}{}_3Mn^{3.75+}{}_4O_{12}$.[9,10] In those compounds the change in the ionic valence in *B*-site Mn drastically modify the magnetic and transport properties. The aliovalent substitution at the *A*-site also change the valence state of not only the *B*-site transition-metal cation but also the *A*'-site transition-metal cation. In $ACu_3V_4O_{12}$ ($A = Na^{+}$, Ca^{2+}, Y^{3+}), the valence states of both the *A*'-site Cu ion and *B*-site V ion change when the *A*-site ion changes.[19] Electrons produced by the *A*-site substitution are doped into both the Cu and V bands, and the Fermi energy in the electronic structure is shifted to the higher energy within a rigid-band picture. In the present $La_{1-x}Na_xMn_3Ti_4O_{12}$ system Ti^{4+} in octahedral coordination with oxygen ions is quite stable and the doping at the *A* site is therefore compensated by the variable valence of Mn ions at the *A'* site.

The present results also strongly suggest the presence of unusual low-valence state of Mn at the square-planer coordinated *A'* site. Although the monovalent Mn ion is not common in oxides, the low-valence like $Mn^{1.81+}$ and $Mn^{1.66+}$ seem to be stabilized in the x = 0.5 and 1.0 samples, respectively. At the initial stage of the experiments, we considered the valence states of the *A*'-site Mn can easily be adjusted by the Mn/Ti mixing. In $LaMn^{1.66+}{}_3Ti^{4+}{}_4O_{12}$, for example, small amount of Mn^{3+} incorporation into the *B* site can increase the valence state of the *A'*-site Mn, and if the mixing reaches $LaMn_3(Ti_{0.75}Mn_{0.25})^{4+}{}_4O_{12}$, the unusual low-valence state $Mn^{1.66+}$ is no more available and a typical Mn^{2+} is stabilized at the square-planer coordinated *A'* site. Indeed, when we made a sample with a nominal composition $LaMn_3(Ti_{0.75}Mn_{0.25})_4O_{12}$, we could also obtain an almost single-phase sample. Although the normal X-ray diffraction results gave no apparent difference between the nominal $LaMn_3T_4O_{12}$ and $LaMn_3(Ti_{0.75}Mn_{0.25})_4O_{12}$ samples, RXS clearly differentiates the two. In contrast that the refined Ti/Mn mixing at the *B* site is 0.992(3)/0.008 for the nominal $LaMn_3T_4O_{12}$, that is 0.727(4)/0.273 for the $LaMn_3(Ti_{0.75}Mn_{0.25})_4O_{12}$ samples, indicating the chemical compositions are very close to the nominal ones. Even with the nominal composition, a mixed valence state in the *B*-site Ti is another way to adjust the neutrality of the compound such as $LaMn^{2+}{}_3Ti^{3.75+}{}_4O_{12}$. Considering the insulating nature of the sample, however, this can be ruled out because the mixed valence state in the *B*-site cation usually induces the conducting property. Our high-pressure synthesis thus appears to help for stabilizing Mn ions with such an unusual low-valence valence state. The

monovalent Mn in oxides was also recently found in $La_{1-x}Ca_xMnO_{2+\delta}$, which was obtained by low-temperature reduction from $La_{1-x}Ca_xMnO_3$ by using sodium hydride[20]. In $La_{1-x}Ca_xMnO_{2+\delta}$ Mn^+ appears to have an unusual tetrahedral coordination. In the present $(La_{0.781}Na_{0.219})^{2.56+}Mn^{1.81+}{}_3Ti^{4+}{}_4O_{12}$ (x = 0.5) and $La^+Mn^{1.66+}{}_3Ti^{4+}{}_4O_{12}$ (x = 1.0) samples, the distorted (split *A'*-site Mn) square-planer coordination should stabilize the unusual low-valence state of monovalent Mn.

The insulating behavior in these compounds with *Im*-3 symmetry suggests random distribution of Mn^+ and Mn^{2+} at the *A*' site, which may well be called "charge-glass state". The magnetic behaviors of $La_{1-x}Na_xMn_3Ti_4O_{12}$ at low temperature are noted and they depend on their valence states of *A*'-site Mn. In $LaMn_3Ti_4O_{12}$ and $NaMn_3Ti_4O_{12}$, the susceptibilities measured on field cooling (FC) and zero-field cooling (ZFC) are different below the temperature much higher than the magnetic transition temperature T_m, whereas the susceptibility shows a typical antiferromagnetic-like peak in $La_{0.78}Na_{0.22}Mn_3Ti_4O_{12}$. The behavior with difference between the FC and ZFC susceptibility for the wide temperature range is typical for spin glass, and the mixture of local magnetic moments, Mn^{2+} and Mn^{3+} for $NaMn_3Ti_4O_{12}$ and Mn^+ and Mn^{2+} for $LaMn_3Ti_4O_{12}$, should cause the spin-glass like behavior. On the other hand, the Mn spins which are close to that of Mn^{2+} in the x = 0.5 sample couple antiferromagnetically below 8 K, though the Mn ion in the sample is in the mixed valence state. The spin-glass like behavior for x = 0, 1 samples should therefore be attributed to the charge-glass state of Mn^+/Mn^{2+} or Mn^{2+}/Mn^{3+} ions at the *A*' site, which may produce random distribution of the magnetic interactions in the *A*' magnetic lattice. For x = 0.5 sample, the Mn valence is close enough to +2 to cause antiferromagnetic transition of Mn spins. Thus, in the $La_{1-x}Na_xMn^{(5+2x)/3}{}_3Ti^{4+}{}_4O_{12}$ system, interestingly, the *A'*-site Mn magnetic property changes from spin-glass like to antiferromagnetism and back to spin-glass like, by changing the Mn valence from +1.66 (x = 0.0) to +2.33 (x = 1.0).

Conclusions

The solid solutions of $La_{1-x}Na_xMn_3Ti_4O_{12}$ were synthesized under high-pressure and high-temperature conditions. From the Rietveld analysis of the synchrotron X-ray diffraction data, it was confirmed that the samples crystallized with the *A*-site-ordered perovskite structures in which the *A*-site Mn ions were slightly displaced from the ideal positions with high site selectivity of Mn/Ti over *A*'/*B* sites. Systematic change in the lattice parameters and BVS values suggests that substituting Na^+ for La^{3+} at the *A* site changed the valence state of the *A'*-site Mn but not that of the

B-site Ti, and the existence of a rare valence state Mn^{+} was strongly suggested for $x = 0$ and $x = 0.5$. *A*' site Mn ions form a charge-glass state, where Mn^{+}/Mn^{2+} or Mn^{2+}/Mn^{3+} is distributed randomly in a static way, which induces spin-glass like behavior in the end compositions $x = 0$ and $x = 1$. Mn^{+} which is very rare for oxides has been stabilized by a high pressure technique, which may open a way to discover novel physical properties in the future.

Acknowledgments

This work was done under the Strategic Japanese-UK Cooperative Program by Japan Science and Technology Agency (JST) and Engineering and Physical Sciences Research Council (EPSRC). The synchrotron X-ray diffraction experiments were performed with the approval of the Diamond Light Source in UK. The work was partly supported by Grants-in-Aid for Scientific Research (Grant Nos. 19GS0207 and 22740227), by the Global COE Program "International Center for Integrated Research and Advanced Education in Materials Science" (No. B-09), by the Project of Integrated Research on Chemical Synthesis from the Ministry of Education, Culture, Sports, Science and Technology (MEXT) of Japan, and by the JST CREST program. Support was also provided by EPSRC and the Leverhulme Trust, United Kingdom.

Reference

[1] Shimakawa, Y. *Inorg. Chem*. **2008**, *47*, 8562.

[2] Vasil'ev, A. N.; Volkova, O. S. *Low Temp. Phys.* **2007**, *33*, 895.

[3] Shiraki, H.; Saito, T.; Yamada, T.; Tsujimoto, M.; Azuma, M.; Kurata, H.; Isoda, S.; Takano, M.; Shimakawa, Y. *Phys. Rev. B* **2007**, *76*, 140403.

[4] Kim, Y. J. Wakimoto, S. Shapiro, S. M. Gehring, P. M.; Ramirez, A. P. *Solid State Communications* **2002**, *121*, 625-629.

[5] Shimakawa, Y. Shiraki, H.; Saito, T. *J. Phys. Soc. Jpn.* **2008**, *77*, 113702.

[6] Long, Y. W.; Hayashi, N.; Saito, T.; Azuma, M.; Muranaka, S.;Shimakawa, Y. *Nature* **2009**, *458*, 60.

[7] Long, Y. Saito, T. Tohyama, T. Oka, K. Azuma, M.; Shimakawa, Y. *Inorganic Chemistry* **2009**, *48*, 8489-8492.

[8] Zeng, Z.; Greenblatt, M.; Subramanian, M. A.; Croft, M. *Phys. Rev. Lett.* **1999**, *82*, 3164.

[9] Alonso, J. A.; Sanchez-Benitez, J.; Andres, A. De.; Martinez-Lope,M. J.; Casais, M. T.; Martinez, J. L. *Appl*. *Phys*. *Lett*. **2003**, *83*, 2623.

[10] Takata, K.; Yamada, I.; Azuma, M; Takano, M.; Shimakawa, Y. *Phys*. *Rev*. *B* **2007**, *76*, 024429.

[11] Marezio, M. Dernier, P. D. Chenavas, J.; Joubert, J. C. *Journal of Solid State Chemistry* **1973**, *6*, 16-20.

[12] Bochu, B. Chenavas, J. Joubert, J. C.; Marezio, M. *Journal of Solid State Chemistry* **1974**, *11*, 88-93.

[13] Imamura, N. Karppinen, M. Motohashi, T. Fu, D. Itoh, M.; Yamauchi, H. *Journal of the American Chemical Society* **2008**, *130*, 14948-14949.

[14] Tohyama, T. Saito, T. Mizumaki, M. Agui, A.; Shimakawa, Y. *Inorganic Chemistry* **2010**, *49*, 2492-2495.

[15] Saito, T. Tohyama, T. Woodward, P. M. Shimakawa, Y. *Bulletin of the Chemical Society of Japan* **2011,** *84*, 802–806.

[16] Long, Y. Saito, T. Mizumaki, M. Agui, A.; Shimakawa, Y. *Journal of the American Chemical Society* **2009**, *131*, 16244-16247.

[17] Topas v3.0: General Profile and Structure Analysis Software for Powder Diffraction Data, Bruker AXS, Karlsruhe, Germany,2000.

[18] Brown, I. D.; Altermatt, D. Acta Crystallogr. **1985**, *B41*, 244.

[19] Shiraki, H. Saito, T. Azuma, M.; Shimakawa, Y. *J. Phys. Soc. Jpn.* **2008**, *77*, 064705.

[20] Dixon, E. Hadermann, J.; Ramos, S. Goodwin, A. L. Hayward, M. A. *J. Am. Chem. Soc*. **2011**, *133*, 18397–18405.

Table 1: Refined structural parameters and selected bond lengths for $La_{1-x}Na_xMn_3Ti_4O_{12}$ obtained from the combined analysis of the resonant and non-resonant X-ray diffraction data. *A*-site La/Na at 2a (0,0,0), *A*'-site Mn at 12e (0.5, *y*, 0.5), B-site Ti at 8c (0.25, 0.25, 0.25) and O at 24g (*x*, *y*, 0). Space group *Im*-3. Numbers in parentheses are standard deviations of the last significant digit. U_{iso} is the isotropic thermal parameter. Bond Valence Sums V_i were calculated from $V_i = \Sigma_j s_{ij}$、 where $s_{ij} = \exp[(r_0-r_{ij})/0.37]$ and r_{ij} is the distance between the *i*th cation and *j*th anion. The r_0 values used were 2.172 Å for La, 1.803 Å for Na, 1.760 Å for Mn, and 1.815 Å for Ti.18[18]

Nominal composition	$LaMn_3Ti_4O_{12}$	$La_{0.5}Na_{0.5}Mn_3Ti_4O_{12}$	$NaMn_3Ti_4O_{12}$
a (Å)	7.59414(1)	7.56259(2)	7.46916(1)
A' **y**	0.45509(9)	0.45544(10)	0.47608 (12)
O1 **x**	0.19200(9)	0.19655(11)	0.18925(9)
O1 **y**	0.29561(9)	0.29763(11)	0.30278(8)
A-site occupancy La/Na	1/0	0.7810(11)/ 0.2190(11)	0/1
B-site occupancy Ti/Mn	0.9919(30)/0.0081(30)	1.0379(43)/-0.0379(43)	0.9433(37)/0.0567(37)
A U_{iso} (100×Å^2)	0.486(4)	0.413(6)	0.275(40)
A' U_{iso} (100×Å^2)	1.352(20)	1.695(20)	0.861(11)
B U_{iso} (100×Å^2)	0.508(5)	0.528(7)	0.609(4)
O U_{iso} (100×Å^2)	1.048(18)	0.844(19)	0.801(12)
A-O(Å)	2.6738(4)×12	2.6974(5)×12	2.6671(3)×12
Mn-O(Å)	2.1552(7)×4	2.1600(8)×4	2.0494(8)×4
	2.5340(8)×2	2.4848(10)×2	2.6005(8)×2
	3.0181(5)×2	2.9880(5)×2	2.9006(8)×2
	3.1004(8)×2	3.0448(9)×2	3.1190(4)×2
	3.4879(5)×2	3.4590(6)×2	3.3670(5)×2
Ti-O(Å)	1.9801(2)×6	1.9666(2)×6	1.9616(2)×6
BVS(*A*)	3.09	---	1.16
BVS(Mn)	1.76	1.79	2.20
BVS(Ti)	3.84	3.98	4.04
R_{WP}	6.06	6.87	6.62
R_B	2.60	3.30	2.15
χ^2	2.90	3.36	2.95

Table 2. Summary of the magnetic properties for $La_{1-x}Na_xMn_3Ti_4O_{12}$. θ and C were obtained from the Curie-Weiss fits of the magnetic susceptibility of the samples. Effective magnetic moments per Mn ion obtained from the Curie constants and those estimated form the refined chemical composition (Table 1) are also listed.

	$LaMn_3Ti_4O_{12}$	$La_{0.78}Na_{0.22}Mn_3Ti_4O_{12}$	$NaMn_3Ti_4O_{12}$
θ (K)	-35	-53	-81
C (emu/mol·K)	11.7	12.2	11.1
Effective magnetic moments p_{eff} (μ_B/Mn):			
Experimental:	5.58	5.69	5.45
Ideal composition:	5.68	5.74	5.68

Figures

Fig. 1. Crystal structure of $AA'_3B_4O_{12}$ perovskites. *A* and *A*' site cations in the ratio of 1:3 are ordered and the *A*'-site ion is square-planar coordinated with oxygen ions. Corner-sharing BO_6 octahedra are heavily tilted.

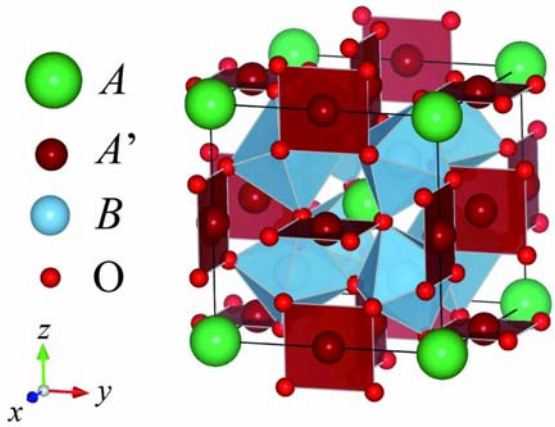

Fig. 2. (a) Non-resonant (λ = 0.82716 Å) and (b) resonant (λ = 1.898161 Å) synchrotron X-ray diffraction patterns and Rietveld analysis results of $LaMn_3Ti_4O_{12}$. Small amounts of impurity phases TiO_2(6.00wt%: Allowed reflections are marked with center ticks.) and $LaMnO_3$(1.88wt%: Allowed reflections are marked with bottom ticks.) were included in the refinement.

(a)

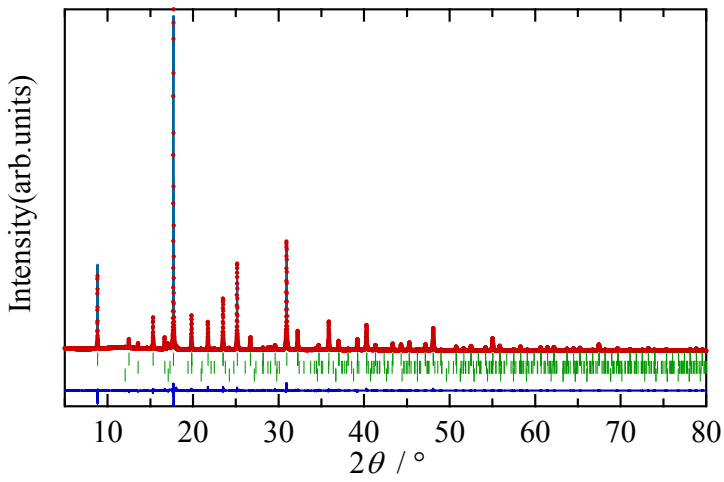

(b)

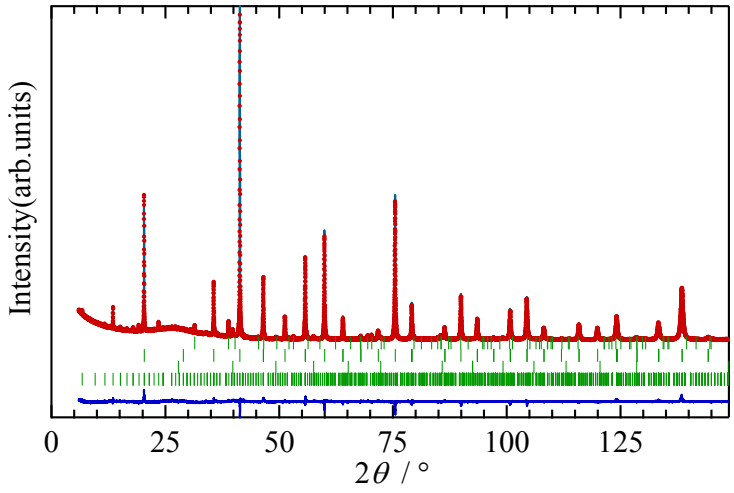

Fig. 3. Lattice constant of $La_{1-x}Na_xMn_3Ti_4O_{12}$ plotted against x. The change in the lattice constant is consistent with Vegard's law. This consistency indicates that the solid solution of $La_{1-x}Na_xMn_3Ti_4O_{12}$ with the refined compositions was successfully synthesized.

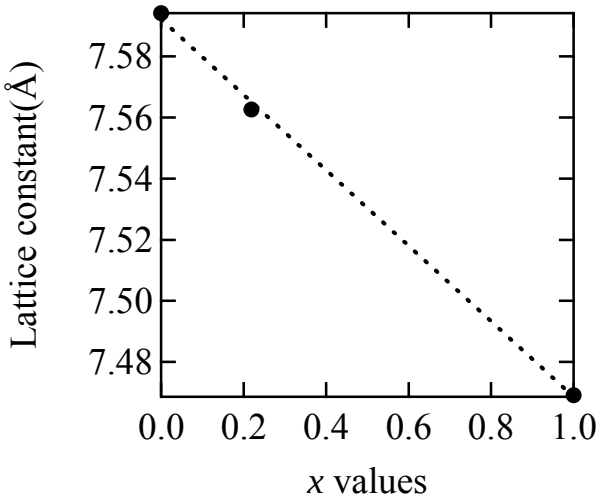

Fig. 4. Temperature dependence of the magnetic susceptibility measured at 1kOe and the inverse susceptibility of $La_{1-x}Na_xMn_3Ti_4O_{12}$.

(a)

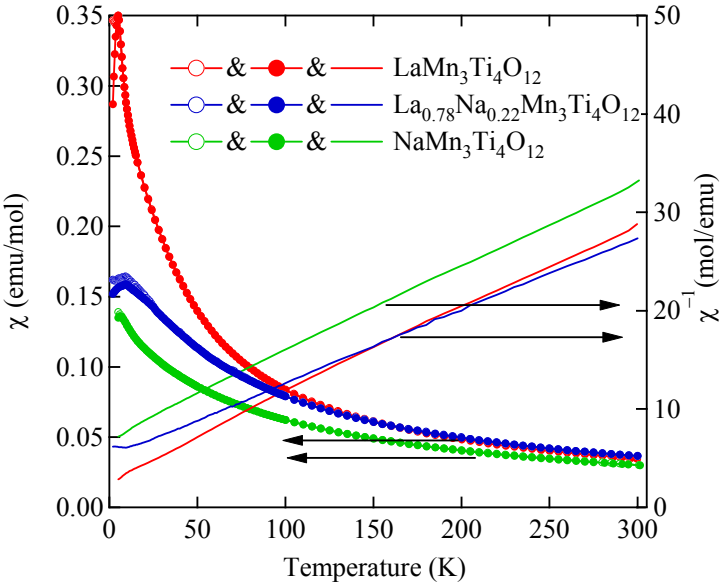

(b)